Modeling Oxygen Dynamics under Variable Work Rate

Alexander Artiga Gonzalez[1], Raphael Bertschinger[2], Fabian Brosda[1], Thorsten Dahmen[1],
Patrick Thumm[2], and Dietmar Saupe[1]

[1]*Dept. of Computer and Information Science, University of Konstanz, Konstanz, Germany*

[2]*Dept. of Sport Science, University of Konstanz, Konstanz, Germany*

{Alexander.Artiga-Gonzalez, Raphael.Bertschinger, Dietmar.Saupe}@uni-konstanz.de

Abstract: Measurements of oxygen uptake and blood lactate content are central to methods for assessment of physical
fitness and endurance capabilities in athletes. Two important parameters extracted from such data of incre-
mental exercise tests are the maximal oxygen uptake and the critical power. A commonly accepted model of
the dynamics of oxygen uptake during exercise at constant work rate comprises a constant baseline oxygen
uptake, an exponential fast component, and another exponential slow component for heavy and severe work
rates. We generalized this model to variable load protocols by differential equations that naturally correspond
to the standard model for constant work rate. This provides the means for prediction of oxygen uptake re-
sponse to variable load profiles including phases of recovery. The model parameters were fitted for individual
subjects from a cycle ergometer test. The model predictions were validated by data collected in separate tests.
Our findings indicate that oxygen kinetics for variable exercise load can be predicted using the generalized
mathematical standard model, however, with an overestimation of the slow component. Such models allow
for applications in the field where the constant work rate assumption generally is not valid.

1 INTRODUCTION

Physiological quantities such as heart rate, lactate concentration, or respiratory gas exchange are important parameters to assess the performance capabilities of athletes in competitive sports. In particular the respiratory gas exchange is a valuable source of information since it allows for a non-invasive, continuous, and precise measurement of the gross oxygen uptake and carbon dioxide output of the whole body. Particularly in endurance sports, the metabolic rates of this substantial fuel and the degradation product of the exercising muscles are reflected in that rate.

Characteristic responses to specific load profiles in different intensity domains have been subject of research effort in recent years (Poole and Jones, 2012; Jones and Poole, 2005). The most distinctive parameters in the description of $\dot{V}O_2$ kinetics are the highest attainable oxygen uptake ($\dot{V}O_{2max}$), the steady-state level with submaximal load, and the rate of increase in $\dot{V}O_2$ at the transition to a higher load level. Basically, the oxygen uptake mechanism may be viewed as a composition of first-order control systems, thus responses to step-shaped load profiles are often described as exponential functions that serve as a regres-

sion to measurement data.

In particular for endurance sports like cycling the models for power demand due to mechanical resistance are well understood. However, the individual power supply model of an athlete is the bottleneck that has hindered the design of an individual adequate feedback control system that guides him/her to perform a specific task such as to find the minimum-time pacing in a race on a hilly track (Dahmen, 2012). For such purposes, a dynamic model for the prediction of gas exchange rates in response to load profiles given by a particular race course would be beneficial.

Stirling et al. (2008) provided a dynamic model. However, it deviates significantly from several theoretical physiological aspects. E.g., it does not consider separate fast and slow components and any delays in the response to heavy and severe work rates. Moreover, it does not provide a model for the steady state oxygen demand as a function of exercise load, and has not been applied to variable load profiles.

We propose that the first step towards dynamical models for variable load should be derived from the established models for constant work rate before more general models are considered and can be compared with the former ones. Therefore, in this contribution,

we generalize the original model equations towards arbitrary load profiles and calibrate and validate them using four load profiles of different characteristics.

2 PREVIOUS WORK

A detailed review and historical account of the mathematical modeling of the $\dot{V}O_2$ kinetics for constant work rate (CWR) has recently been given by Poole and Jones (2012), containing over 800 references. See also Jones and Poole (2005) and, for a clarification, Ma et al. (2010). Therefore, here we only briefly summarize the established model as far as necessary for an understanding of our generalization and refer to the above mentioned works for further explanations and references to literature.

According to the commonly accepted and widely applied model the $\dot{V}O_2$ kinetics can be separated into four distinct components.

- Baseline component. This constant component accounts for the oxygen consumption at rest, i.e., for the time prior to the onset of exercise.

- Rapid, initial increase (Phase I). At the start of the exercise a rapid but small initial increase of $\dot{V}O_2$ occurs and is completed within the first 20 s.

- Primary, fundamental, or fast component (Phase II). This phase is characterized by a (typically larger) exponential increase of $\dot{V}O_2$ with a time constant of 20–45 s. After saturation and for given work rate below the lactate threshold, this component represents the required steady-state demand of oxygen.

- Secondary, slow component (Phase III). The slow component occurs only for work rates above the lactate threshold. It brings in an additional increase of $\dot{V}O_2$ to a total that for severe work rates above the critical power is roughly equal to the maximal oxygen consumption, $\dot{V}O_{2max}$.

Each of the components in Phases I to III are modeled as exponential functions of type

$$A\left(1 - \exp\left(-\frac{t-T}{\tau}\right)\right) \quad (1)$$

where time is denoted by t and with different amplitudes A, time delays T, and time constants τ, see Figure 1. The time constant τ determines the time required for the dynamics of the corresponding component to diminish the difference with the asymptotic amplitude A by a factor of $1 - 1/e \approx 0.632$. Thus, after a time of 3τ about 95% of the amplitude A is realized and the corresponding phase is regarded as
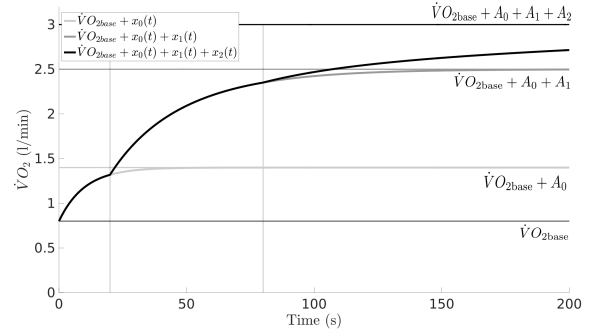

Figure 1: Steady-state dynamics consisting of a baseline component $\dot{V}O_{2base}$ together with three exponentially asymptotic functions $x_0(t)$, $x_1(t)$ (fast component), and $x_2(t)$ (slow component) of different amplitudes, decay rates, and delays.

effectively having reached its final value. It is important to take note that the time delay T is intended to imply that only after that time the oxygen consumption of the corresponding component is beginning. To complete the model, we therefore apply the Heaviside step function (Ma et al., 2010)

$$H(t) = \begin{cases} 1, t \geq 0 \\ 0, t < 0 \end{cases} \quad (2)$$

setting

$$x_k(t) = A_k\, H(t - T_k)\left(1 - \exp\left(-\frac{t - T_k}{\tau_k}\right)\right) \quad (3)$$

yielding the complete model in one formula as

$$\dot{V}O_2(t) = \dot{V}O_{2base} + \sum_{k=0}^{2} x_k(t). \quad (4)$$

Here, $\dot{V}O_{2base}$ is the baseline component, and the index $k = 0, 1, 2$ refers to the components of the three phases, which are parametrized by their corresponding amplitudes A_k, time delays T_k, and time constants τ_k. In Phase I there is no delay; $T_0 = 0$. This is the standard form of oxygen dynamics and illustrated in Figure 1.

Phase I typically lasts only a couple of breaths until reaching its target amplitude A_0 and during this short period of time at the onset of exercise there is a large variability of the inter breath gas exchange making it difficult to fit a model to an individual ventilatory data series (Whipp et al., 1982). Therefore, many researchers remove that time period from the data and consider only the first, fast response and the second, slow component (Jones and Poole, 2005, page 26). The baseline amplitude would then have to be incremented by the amplitude A_0 to compensate for the deletion of Phase I. In this study we also follow

this procedure. Thus, from here on, $\dot{V}O_{2\text{base}}$ refers to the above mentioned baseline component (renamed as $\dot{V}O_{2\text{min}}$ and measured directly) plus an estimated add-on accounting for A_0.

In this kinetic model of $\dot{V}O_2$ consumption for constant work rate the amplitudes A_k must be chosen adaptively. They depend on the physiological and metabolic condition of the subject and on the applied constant work rate P. Thus, $A_k = A_k(P)$. As a first approximation the amplitude of the first, fast component can be taken as a linear function of exercise intensity (power), with slope of 9–11 ml/min per Watt of power increase and bounded by $\dot{V}O_{2\text{max}}$ (Poole and Jones, 2012, page 939).

The second, slow component is more complex. It is the sum of two parts. The first part is an increasing function, which seems to start having nonzero values from about the lactate threshold up to the value of critical power P_c, where the sum of all components is still less than $\dot{V}O_{2\text{max}}$. The exact form of this function has not been determined. For power greater than critical power the slow component for constant work rate exercise eventually raises the total oxygen consumption up to $\dot{V}O_{2\text{max}}$. Thus, for $P > P_c$, it can be modeled as an affine linear, decreasing function which is the difference between $\dot{V}O_{2\text{max}}$ and the sum of the amplitudes of the baseline and first, fast component.

This model has been validated with CWR and also incremental exercise, where the slow component is not or at least not fully apparent. In the following section we propose a concrete parametrized model of the total oxygen consumption following these findings, summarized in Figure 5.

3   METHODS

Experimental setup

Five healthy, recreationally to well trained subjects (age 37.8±14.8 yrs, height 180.4±10.1 cm, weight 75.2±7.6 kg) gave written informed consent to take part in the study and were thoroughly informed about the testing procedure. The subjects completed four different cycle ergometer (Cylus2, RBM elektronik-automation GmbH, Leipzig, Germany) tests with continuous breath-by-breath gas exchange and ventilation measurements at the mouth (Ergostik, Geratherm Respiratory GmbH, Bad Kissingen, Germany). The tests were designed to determine a set of necessary physiological parameters of aerobic capacity ($\dot{V}O_{2\text{max}}$, ventilatory threshold 1 (VT_1) and maximal lactate steady state (MLSS)). Furthermore the tests featured a variety of load profiles in order to comprehensively evaluate the model prediction quality.

The following paragraphs describe the four test protocols in detail. See Figures 2 and 3 for a visualization of the corresponding work rate and road gradient profiles.

Test 1   (see Figure 2, top)
The testing procedure commenced with an incremental step test starting at a workload of 80 W with increments of 20 W every 3 minutes. In the initial step the subjects were instructed to choose their preferred cadence between 80–100 rpm and were then instructed to keep the cadence constant in all four test trials. The step test was terminated at volitional exhaustion of the subject. After test termination subjects recovered actively at 80 W and at or near their self-selected cadence for five minutes. In this test, additionally to gas exchange recordings, blood lactate measurements (Lactate Pro 2, Arkray Factory Inc., Shiga, Japan) were sampled to determine the MLSS. Lactate probes from the earlobe (0.3 µl) were taken at the end of every step, at volitional exhaustion of the subject as well as 1, 3, and 5 minutes after test termination. Physiological parameter determination is explained in detail in the next subsection below.

Test 2   (see Figure 2, bottom)
The second ergometer test consisted of four sprints of 6 s duration each and an incremental ramp test. Two sprints were carried out before and two after the ramp test to obtain the subjects' maximal power output and $\dot{V}O_2$ profiles in a recovered and a fatigued state. Before each set of sprints subjects pedaled at 80 W for 5 minutes at their self-selected cadence. The two sprints of each set were separated by 30 s of passive rest and subsequent 2 min 24 s of active recovery at 80 W. The ergometer load for the sprints was calculated on the basis the subjects' body weight multiplied by a factor of 5, expressed in Newton. Ten seconds before each sprint subjects were instructed to increase their cadence gradually in order to obtain their maximal pedaling frequency directly at the start of the sprint when the load was applied to the flywheel of the ergometer. The subjects were able to time their effort by a countdown visually presented on a large screen.

In order to obtain approximately the same ramp test time of 10 minutes for every subject, the end load of the ramp protocol was estimated individually by the highest exercise intensity reached in the incremental step test multiplied by a factor of 1.3. The start load was set to 80 W, hence the increment per minute was obtained by the following formula: (Individual end load of step test in Watt − start load of 80 W) / 10 minutes. Workload was increased every second until the subject terminated the test volitionally.
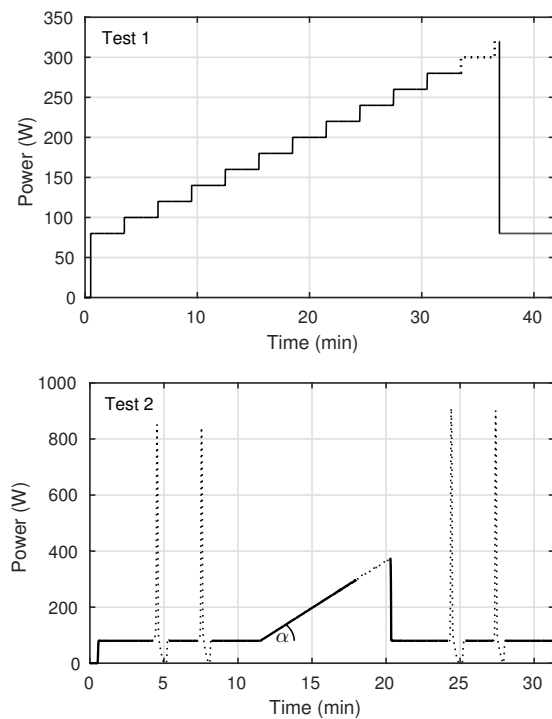
Figure 2: Test protocols of the first (top) and second (bottom) cycle ergometer test (see text for details). Dashed lines indicate individual variability in maximal power output achieved during the test. The angle α indicates individual variability in the calculated slope of the workload increase.

Test 3 (see Figure 3, top)

In the third test subjects had to complete a variable step protocol. The steps varied in load and duration and alternated between low and moderate or severe intensity. The linearly in- or decreasing intensity between the steps was also varied in time. The intensities were calculated in relation to the MLSS. In short, the step protocol looked as follows: 4 min at 80 W, 4 min at 75% MLSS, 2 min at 40% MLSS, 2 min at 95% MLSS, 2 min at 45% MLSS, 4 min at 85% MLSS, 3 min at 90 W, 2 min at 100% MLSS, 5 min at 80 W, 2 min at 105% MLSS, 2 min at 70 W, 1 min at 60% MLSS, and 2 min at 80 W. Fixed workloads for some intervals have been used because the ergometer was not able to handle workloads that were below 40% of MLSS for some subjects. Subsequently, a constant load all-out exercise at 140% MLSS followed. This interval lasted from 1.5 to 4.5 minutes between subjects. The final interval was designed as a recovery ride at 80 W for 5 minutes.

Test 4 (see Figure 3, bottom)

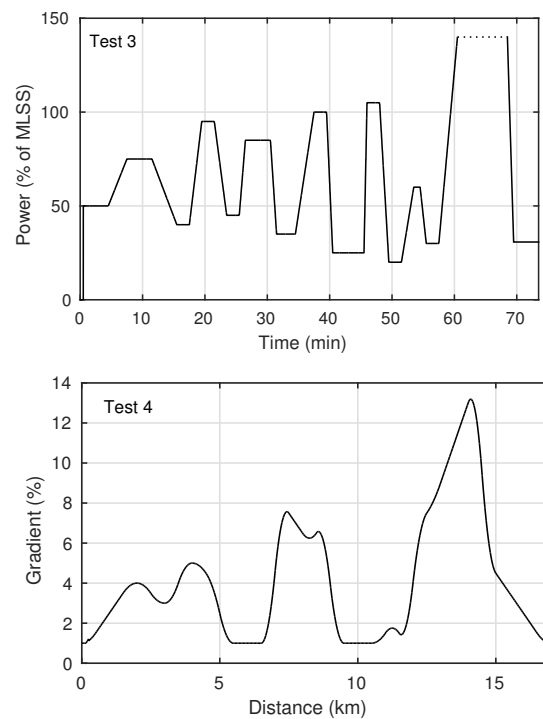For the final "synthetic hill climb test" the ergome-

Figure 3: Test protocols of the third (top) and fourth (bottom) cycle ergometer test (see text for details). The dashed line in Test 3 indicates individual variability of time achieved at 140% of MLSS workload.

ter was controlled by our simulator software (Dahmen et al., 2011). The load was defined by a mathematical model (Martin et al., 1998) to simulate the resistance on a realistic track. The gradient of that track, depicted in Figure 3, and the subjects' body weight were the major determinants of the load. While holding the same cadence as before, the subjects were able to choose their exercise intensity by gear shifting. (On the steepest section most subjects were not able to hold the cadence even in the lowest gear.)

Before each session the gas analyzers were calibrated with ambient air and a gas mixture of known composition (15% O_2, 5% CO_2 and N as balance). The flow sensor was calibrated by means of a 3 liter syringe. For an adequate recovery, test sessions were separated by at least 48 hours. Subjects were instructed to visit the laboratory in a fully recovered state and were asked to refrain from intense physical activity two days prior testing. In all test sessions subjects received strong verbal encouragement from the investigators when they were in reach of their physical limits. During all experiments subjects were aware of relevant mechanical variables like power and cadence displayed on a large screen. Cadence was held constant throughout all tests except the sprints in Test 2

and the steep sections (>10% gradient) of Test 4. To obtain a minimal $\dot{V}O_2$ ($\dot{V}O_{2\text{min}}$) value, subjects stayed seated for 30 s on the ergometer before the start of each test.

Physiological parameter determination

MLSS was determined on the basis of the incremental step test. For clarity MLSS is used here interchangeably with the term critical power (P_c) as it has been shown to occur broadly at the same workload (Vautier et al., 1995). However, this finding is not unanimous as, e.g., Pringle and Jones (2002) have found that the MLSS underestimated critical power by about 20 W in their studies.

The MLSS is defined as "the exercise intensity that is associated with a substantial increase in blood lactate" (Svedahl and MacIntosh, 2003, page 300), hence it was determined as the workload before an increase in lactate concentration of at least 1/10th of the maximal lactate concentration (reached at the test abortion or in the recovery phase) could be observed. The step before this substantial blood lactate increase was chosen for the MLSS intensity, see Figure 4.

To set the corresponding critical power P_c, we added ±3 W to the power at MLSS, depending on the amount of increase before and after the MLSS in order to avoid having a workload in the tests that oscillates around the critical power P_c at which point the steady-state model for oxygen demand has a discontinuity as explained in the next subsection.
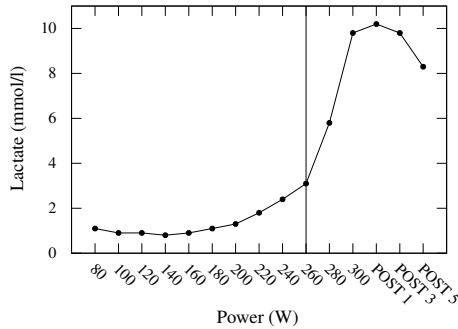

Figure 4: Example for the method of determining MLSS in the lactate curve for Subject 5.

VT_1 was determined visually on the basis of the ramp protocol in Test 2. The method used is described in detail in (Beaver et al., 1986). Briefly, plots of VE/VCO_2, VE/VO_2, end-tidal PCO_2 ($PETCO_2$), end-tidal PO_2 ($PETO_2$) and respiratory exchange ratio (RER) vs. time were analyzed. The first criterium for VT_1 is an increase in the VE/VO_2 curve after it has declined or stayed constant, without an increase in

Table 1: Parameters extracted from ergometer tests.

Param.	Unit	Description	Mean$\pm\sigma$
$\dot{V}O_{2\text{min}}$	l/min	minimal $\dot{V}O_2$	0.354 ± 0.070
VT_1	W	first vent. thresh.	183 ± 26
$\dot{V}O_{2\text{max}}$	l/min	maximal $\dot{V}O_2$	4.708 ± 0.873
P_c	W	critical power	260 ± 71

VE/VCO_2. The second criterium is a slowly rising or constant $PETCO_2$ curve together with a beginning in the rise of the $PETO_2$ curve after it has followed a flat or declining shape. The third criterium is a marked increase in RER after following a horizontal or slowly rising shape.

$\dot{V}O_{2\text{max}}$ was determined as the highest $\dot{V}O_2$ of a 10-value moving average obtained in any of the four tests. In 4 out of 5 subjects the test with the highest $\dot{V}O_{2\text{max}}$ was the ramp test. The other subject reached $\dot{V}O_{2\text{max}}$ in the incremental step test.

$\dot{V}O_{2\text{min}}$ was determined as the lowest $\dot{V}O_2$ value obtained during the 30 s resting phase in any of the four ergometer tests.

The steady-state oxygen demand model

Following the model assumptions from the literature as summarized in Section 2 we propose a steady state oxygen demand given by a constant baseline component, the first, fast component, and the second, slow component with amplitudes $\dot{V}O_{2\text{base}}$, $A_1(P)$, and $A_2(P)$, respectively. The exact form of the slow component for loads below the critical power is not specified in the literature and we propose an exponential function, parametrized by its amplitude and growth rate. In terms of formulas, the amplitudes are

$$A_1(P) = \min(s \cdot P,\ \dot{V}O_{2\text{max}} - \dot{V}O_{2\text{base}}) \qquad (5)$$

$$A_2(P) = \begin{cases} V_\Delta \cdot \exp(-(P_c - P)/\Delta) & P \le P_c \\ \dot{V}O_{2\text{max}} - \dot{V}O_{2\text{base}} - A_1(P) & P > P_c \end{cases} \qquad (6)$$

where s is the slope (or gain) for the fast component of about 9–11 ml/min/W, P_c denotes the critical power, V_Δ is the maximal amplitude of the slow component for exercise load up to critical power, and Δ is the corresponding decay constant that governs the decay of the steady-state slow component as the load is decreased from the critical power. Figure 5 depicts the graph of the sum of all components in this model.

The parameters for this steady state oxygen demand model were determined directly from ergometer tests ($\dot{V}O_{2\text{max}}$ and P_c, see Table 1) or by least squares fitting to data from one or more ergometer tests ($\dot{V}O_{2\text{base}}, s, V_\Delta$, and Δ, see Table 2). For the fitting procedure appropriate search ranges for the parameters are also specified in Table 2. These ranges are based on experimental evidence ($\dot{V}O_{2\text{base}}$, Δ) or
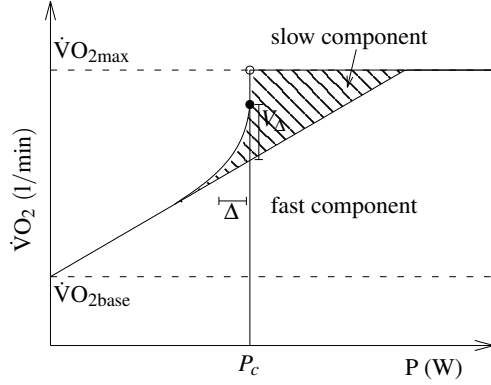
Figure 5: Model of the steady state oxygen demand for the baseline, fast, and slow components.

Table 2: Summary of parameters for the model of the steady state oxygen demand. We set the value for the upper limit of the slow component amplitude, $V_{\Delta max} = \dot{V}O_{2max} - \dot{V}O_{2base} - sP_c$.

Param.	Unit	Description	Range
$\dot{V}O_{2base}$	l/min	baseline $\dot{V}O_2$	$[\dot{V}O_{2min}, 1.0]$
s	l/min/W	exercise economy	$\left[\frac{\dot{V}O_{2max}}{4 \cdot P_c}, \frac{\dot{V}O_{2max}}{P_c}\right]$
V_Δ	l/min	ampl. slow comp.	$[0, V_{\Delta max}]$
Δ	W	range slow comp.	$[0, P_c - VT_1]$

by constraints of the model. E.g., the upper bound $\dot{V}O_{2max}/P_c$ for the slope s stems from the extreme case where $\dot{V}O_{2base} = 0$ and $\dot{V}O_2(P_c) = \dot{V}O_{2max}$.

Dynamic model of oxygen consumption

Now let us extend the steady state oxygen demand model so that it becomes dynamic allowing for a variable load profile $P(t)$. The response of the fast and slow component in the case of a constant work rate demand is given by Eq. (1), $A\left(1 - \exp\left(-\frac{t-T}{\tau}\right)\right)$. Note that this function is the solution to the linear ordinary differential equation initial value problem

$$\dot{x} = \tau^{-1}(A - x), \quad x(0) = 0 \qquad (7)$$

however, delayed by the delay time T or, equivalently, the solution for initial value $x(T) = 0$. This suggests the following equations for the first and second component, $x_1(t), x_2(t)$,

$$\dot{x}_k = \tau_k^{-1}(A_k(P) - x_k), \quad x_k(T_k) = 0, \quad k = 1, 2 \qquad (8)$$

defined for times $t \geq T_k$ (and setting $x_k(t) = 0$ for $t < T_k$). Here, the power demand is a function of time $P = P(t)$ and $A_k(P), k = 1, 2$, are the steady state amplitudes for the fast and slow components given in Eqs. (5,6). The total $\dot{V}O_2$ accordingly is given by

$$\dot{V}O_2(t) = \dot{V}O_{2base} + x_1(t) + x_2(t). \qquad (9)$$

Table 3: Parameters for the dynamic model of oxygen consumption. Together with the model for steady state oxygen demand there are 10 parameters to be estimated.

Param.	Unit	Description	Range
τ_1	s	time constant fast comp.	$[20, 45]$
τ_2	s	time constant slow comp.	$[120, 240]$
T_1	s	time delay fast comp.	$[0, 20]$
T_2	s	time delay slow comp.	$[60, 150]$

The differential equations require the four parameters τ_1, τ_2, T_1, and T_2 that are listed together with their corresponding ranges in Table 3. These ranges are set in accordance with empirical findings reported in the survey article of Jones and Poole (2005).

We remark that the above $\dot{V}O_2$ model does not distinguish on- and off-transient dynamics, i.e., the $\dot{V}O_2$ demand and time constants are the same regardless of whether the current $\dot{V}O_2$ value is below (on-transient case) or above the $\dot{V}O_2$ demand (off-transient case). There is, however, some evidence for an asymmetry of dynamics in some of the exercise intensity domains, although this has received little attention in the literature (Poole and Jones, 2012, p. 940). For simplicity, in this contribution we stay with the symmetric model and leave the modeling of asymmetric dynamics for future work.

Data preprocessing

In order to estimate the ten parameters of the dynamic model given by Eqs. (5,6,8) for a particular subject, data series of time-stamped values of produced power and resulting breath-by-breath oxygen consumption are required for exercise intensities ranging from moderate to severe. These time series from ergometer laboratory experiments are typically very noisy, have different sampling rates for $\dot{V}O_2$ and power, and samples may be irregularly spaced.

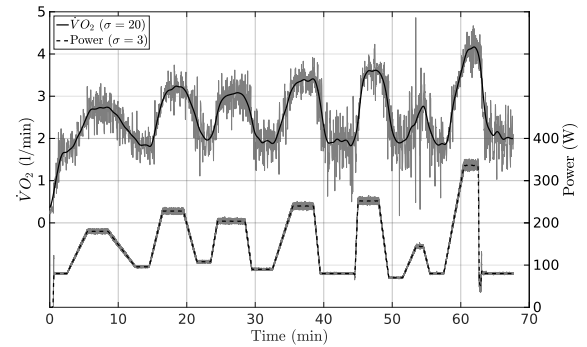Therefore, a combined smoothing and resampling operator has to be applied before param-

Figure 6: Data filtering for ventilatory and power data.

Table 4: Root-mean-square errors of model fit. Parameters have been fitted for each case separately. The approximation quality is expressed by root-mean-square error (rms), maximum error (max), and signal-to-noise ratio (snr). For each subject the best rms, max, and snr values are highlighted in bold font.

	Test 1			Test 2			Test 3			Test 4			Average		
	rms	max	snr	rms	max	snr	rms	max	snr	rms	max	snr	rms	max	snr
	l/min	l/min	dB	l/min	l/min	dB	l/min	l/min	dB	l/min	l/min	dB	l/min	l/min	dB
Subject 1	**0.10**	**0.59**	**32.0**	0.41	1.25	17.7	0.17	0.71	26.3	0.28	0.76	23.4	0.24	0.83	24.8
Subject 2	0.20	0.94	23.2	0.20	0.80	22.2	**0.13**	**0.65**	**26.2**	0.35	0.89	19.3	0.22	0.82	22.7
Subject 3	0.17	**0.49**	23.4	0.18	0.61	21.7	**0.12**	0.55	**24.7**	0.38	1.00	17.0	0.21	0.66	21.7
Subject 4	**0.15**	0.66	**25.2**	0.17	0.64	22.2	0.26	1.16	19.1	0.30	**0.63**	19.9	0.22	0.77	21.6
Subject 5	0.23	1.12	22.2	0.24	0.90	21.0	**0.17**	**0.54**	**24.1**	0.40	0.81	18.9	0.26	0.84	21.6
Average	**0.17**	0.76	**25.2**	0.24	0.84	21.0	**0.17**	**0.72**	24.1	0.34	0.82	19.7	0.23	0.79	22.5

Table 5: Parameters of the fitted model for the subjects from Test 3.

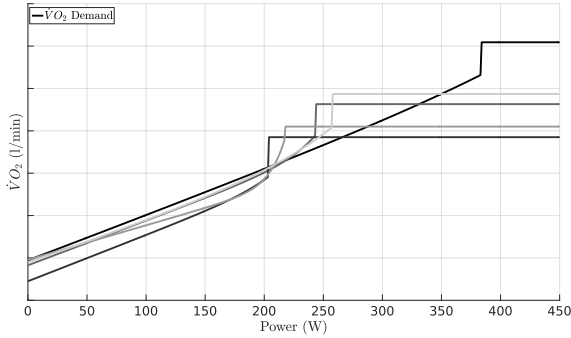| Parameter	$\dot{V}O_{2\text{max}}$	$\dot{V}O_{2\text{base}}$	s	P_c	V_Δ	Δ	T_1	τ_1	T_2	τ_2
Unit	l/min	l/min	l/min/W	W	l/min	W	min	min	min	min
Subject 1	6.09	0.94	10.6×10^{-3}	383	0.33	98	0:04.9	0:32.2	2:38.5	3:34.4
Subject 2	4.63	0.83	10.5×10^{-3}	243	0.50	24	0:04.1	0:29.8	2:41.7	3:17.4
Subject 3	3.85	0.45	10.9×10^{-3}	203	0.24	24	0:06.6	0:29.0	2:42.2	3:42.2
Subject 4	4.10	0.96	8.1×10^{-3}	217	1.05	13	0:02.2	0:21.2	1:04.6	3:50.7
Subject 5	4.87	0.89	9.7×10^{-3}	257	0.71	56	0:06.6	0:28.2	1:16.8	3:24.7

Figure 7: Fitted models of steady state oxygen demand for the five subjects.

eter estimation. In this study we have used the standard Gaussian smoothing filter with kernel $(\sigma\sqrt{2\pi})^{-1}\exp(-0.5t/\sigma^2)$ and $\sigma = 20\,\text{s}$ and $3\,\text{s}$ for respiratory and power measurements, respectively. The filter was applied at time instants uniformly spaced at 1 s intervals. Figure 6 gives an example of measured time series and their smoothed and resampled version.

Parameter estimation

Parameter estimation was done by least squares fitting, minimizing mean squared error between computed model values and the (smoothed) $\dot{V}O_2$ data. Testing has shown that fitting versus the smoothed $\dot{V}O_2$ data produced better results than against noisy measured data. Non-linear least squares fitting may suffer from the presence of many local minima. Thus,

commonly applied optimization algorithms like the downhill simplex method typically get stuck in these and results largely depend on the choice of initial parameters. Thus, we adopted a genetic algorithm (from MATLAB®) which provided better minima by use of its stochastic elements.

Model validation

We calculated model parameters for each ergometer test of each participating subject. To express the quality of the model fit to the data we computed the root-mean-square differences. To validate the predictive power of the model we selected Test 3 for each subject for parameter fitting, and used the other tests for comparing the model predictions of oxygen consumption with the measured values.

4 RESULTS

The $\dot{V}O_2$ model as given by Eqs. (5,6,8,9) was fitted to the data for all four tests and five subjects, resulting in 20 sets of model parameters. The corresponding model errors were calculated by solving the initial value problems (8) and summing up the components according to Eq. (9). The resulting model errors are given in Table 4.

Overall, the average $\dot{V}O_2$ modeling rms error was $0.23 \pm 0.08\,\text{l/min}$. Figure 8 illustrates the $\dot{V}O_2$ and power data, and the fitting result for Subject 2, whose average rms error is the median of errors for subjects.
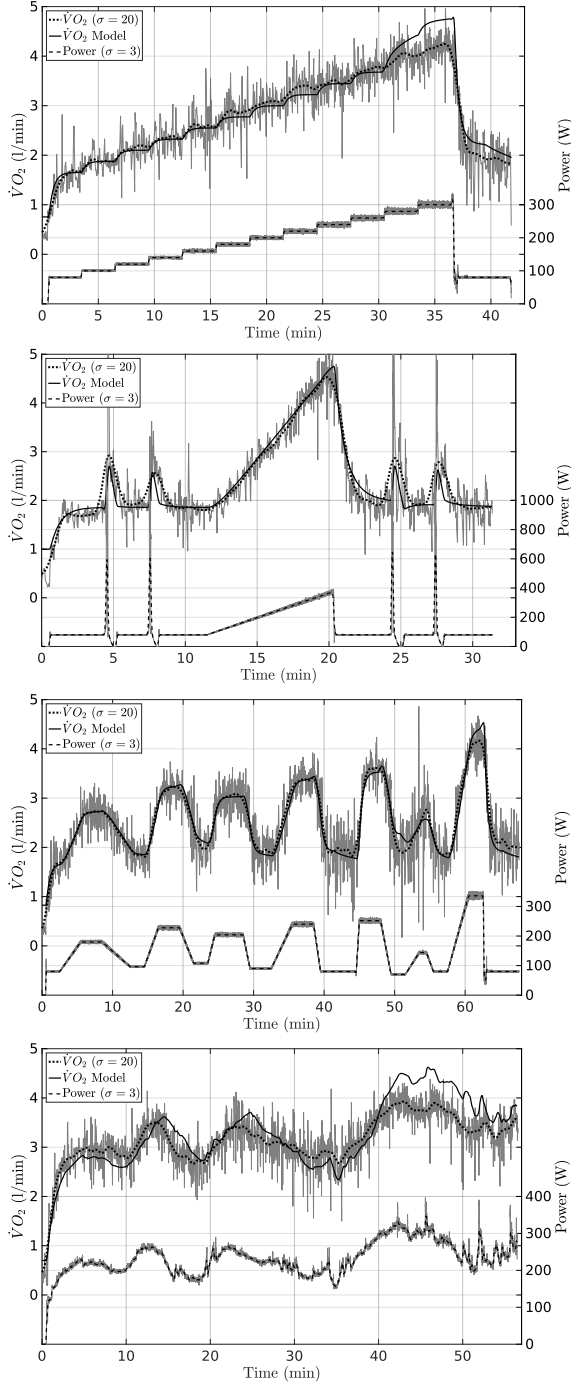
Figure 8: $\dot{V}O_2$ fitting for Subject 2 on all four tests. The lower curves show the power, and the upper two parts depict the recorded and the best fitting $\dot{V}O_2$ curves. The noisy grey signals are the original (unfiltered) measurements.

In the modeling phase, we find that Test 3 performed best, with the smallest average $\dot{V}O_2$ rms error of 0.17 l/min. The corresponding parameter sets for

Table 6: Root-mean-square errors of model predictions for the three tests in the validation set.

	Test 1 l/min	Test 2 l/min	Test 4 l/min	Average l/min
Subject 1	0.19	0.59	0.44	0.41
Subject 2	0.26	0.30	0.50	0.35
Subject 3	0.20	0.33	0.43	0.32
Subject 4	0.25	0.27	0.40	0.31
Subject 5	0.30	0.36	0.78	0.48
Average	0.24	0.37	0.51	0.37

each of the subjects are given in Table 5 and visualized in Figure 7.

In the validation we used the parameters resulting from the model fitting using Test 3 for the prediction of the $\dot{V}O_2$ consumption in the other tests. For the model simulation we used the measured power as input for the differential equations. We recorded the corresponding rms prediction errors in Table 6.

Figures 10 and 11 visualize the prediction of the $\dot{V}O_2$ model. We present the graphs of the $\dot{V}O_2$ prediction and the measured $\dot{V}O_2$ against time for the incremental Test 1 and Test 4, where subjects were self-pacing themselves. Note, that the model prediction errors are mostly positive, i.e., the model overestimated the actual $\dot{V}O_2$ consumption, especially at times of severe exercise intensity.

5 DISCUSSION

Overall, the results show that in principle the approach to transfer the dynamic steady-state model from constant work rates to variable work rates was successful. Parameters could be estimated such that measured $\dot{V}O_2$ data could be approximated with a small rms error of about 0.23 l/min. For model prediction the average error was around 0.37 l/min. The results are even better for work rates in the moderate to heavy exercise intensity domain, as can be seen in Figures 8 and 10.

To illustrate and discuss the dynamics of the differential equation model for the oxygen dynamics we provide Figure 9 that visualizes the total oxygen consumption and the corresponding slow component, both with respect to the oxygen demand, $\dot{V}O_{2\text{base}} + A_1(P(t)) + A_2(P(t))$ and $A_2(P(t))$, respectively, and the modeled responses of the system, $\dot{V}O_2(t), x_2(t)$. Moreover, the corresponding oxygen consumption measurements as well as the applied power $P(t)$ is included. The exponential asymptotic dynamics for piecewise constant demands are clearly visible. Also note the delayed reaction, especially of the slow component. A large oxygen demand in the slow compo-
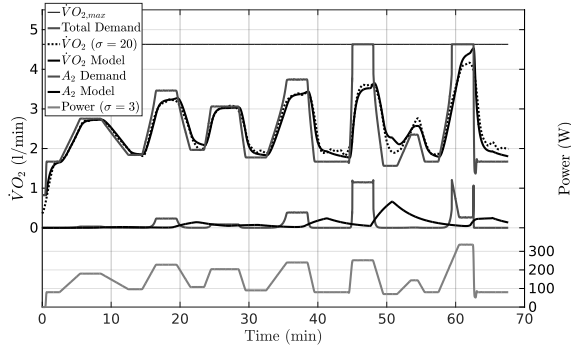
Figure 9: Steady-state demand and dynamic model for Subject 2 on Test 3. See text for details.

Figure 11: $\dot{V}O_2$ model prediction for Test 1 for all five subjects (from Subject 1 at the bottom to Subject 5 at the top), based on parameters gained from parameter estimation on Test 3.

nent may trigger a delayed overcompensation, leading total $\dot{V}O_2$ estimates that are to too large, e.g., near $t = 50$ min.

Therefore, for severe work rates it seems that the model overestimates the slow component, leading to excess $\dot{V}O_2$ contributions. This can be clearly seen in Figure 8 (bottom graph) at about 40 to 50 minutes in the test. During the whole 10 minutes the modeled $\dot{V}O_2$ demand was above the critical power (243 W). There, the slow component drove the modeled $\dot{V}O_2$ towards $\dot{V}O_{2\mathrm{max}}$, while the measured $\dot{V}O_2$ stayed about half a liter per minute below that.

A possible explanation of this artifact is that the estimation of the critical power by MLSS may have been too small due to an imprecise empirical MLSS estimate, or because in our cases the critical power was significantly above the MLSS, as in the experiments of Pringle and Jones (2002), already mentioned before. Another possibility is that the slow component generally is not well understood yet, thereby having led to an inadequate steady state model upon which our model is based. This limits the dynamic phenomena that can be captured to those that are known and were described in the literature. More-
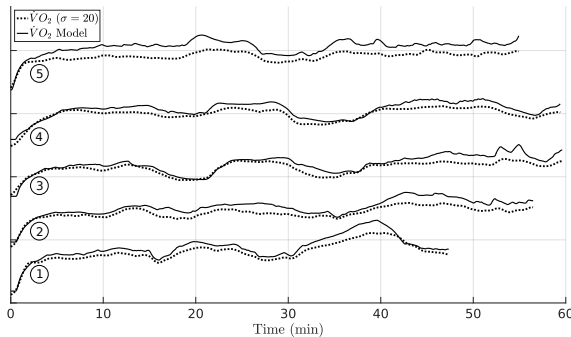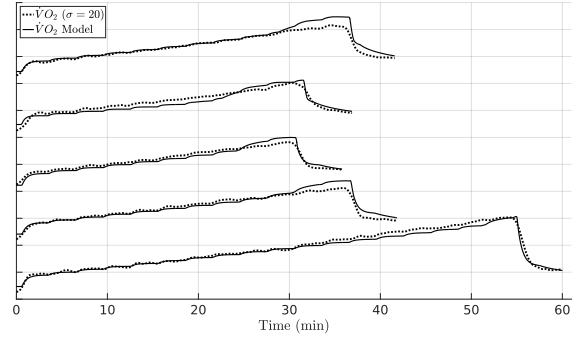
over, some findings or assumptions about the type of functional dependencies are controversial, in particular regarding the slow component, see (Poole and Jones, 2012, page 953). For example, it is not clear at all, that the slow component in constant work rate exercise tests at heavy and severe work rates is asymptotically exponential as expressed in Eq. (1) (Gaesser and Poole, 1996, pages 43, 44).

Therefore, instead of enforcing the slow component one might conjecture that a dynamic model that discards the slow component would yield better prediction results. In order to check this in a quick test, we zeroed the slow component in the parameter fitting procedure. The results for prediction of Test 4 are shown in Figure 12, compare with Figure 10. We see that the results indeed look better than with the slow component for most of the model predictions. However, for the other validation tests the predictions using the slow component are better. Still, this indicates that there is a good opportunity for improvements of the mathematical model beyond the direct transfer from constant to variable work rates.
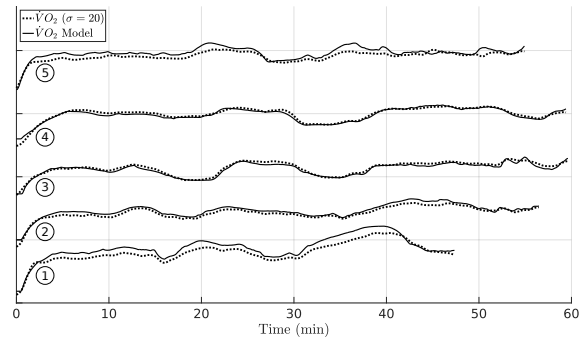

Figure 10: $\dot{V}O_2$ model prediction for Test 4. The curves are given for Subjects 1 to 5 from bottom to top, respectively.

Figure 12: $\dot{V}O_2$ model prediction for Test 4 as in Figure 10. Here, the model was trained *without* the slow component.

6 CONCLUSIONS AND FUTURE WORK

We contributed to the generalization of the commonly accepted model of the dynamics of oxygen uptake during exercise at constant work rates to variable load protocols by means of differential equations. We showed how parameters in the model can be estimated and that the mathematical dynamical model can be used to predict the oxygen consumption for other given load profiles. We found for five subjects and four very different test protocols (of up to about one hour length) that on average the modeling rms error of $\dot{V}O_2$ was 0.23 ± 0.08 l/min and the prediction rms error in three tests was 0.37 ± 0.16 l/min.

The model overestimated the slow component, however. Therefore, we plan to let the critical power be a parameter that can be fitted to training data instead of using the MLSS as an estimate. For such a study the MLSS can serve as a lower limit of the allowable range of values for critical power.

Moreover, a closer study of the slow component in a set of constant work rate (CWR) tests should be carried out by our five subjects. From such lab tests one can also compare the modeling error for the variable work load exercises undertaken for this contribution with those for CWR tests in order to gain an understanding of how much of the modeling precision of CWR carries over to the variable work load case when using the direct generalization of the mathematical modeling as given in this paper.

An alternative approach to modeling would be to allow for different, more appropriate degrees of freedom in the mathematical model, again fitting the model type and parameters to empirical data, and calculating model and prediction errors. For example, we may assume as above two additive model components (besides a constant baseline oxygen consumption) with different delay times and decay rates, however, with corresponding steady state oxygen demands that are restricted only by requiring (piecewise) monotonicity and that can be parametrized by a set of six parameters, the same number as in this contribution.

With such an approach, we expect a better data fitting. It remains open whether also the predictive power is better than for our current model and whether the results can be interpreted in harmony with the current understanding of sport physiology and sport medicine.

REFERENCES

Beaver, W. L., Wasserman, K., and Whipp, B. J. (1986). A new method for detecting anaerobic threshold by gas exchange. *Journal of applied physiology*, 60(6):2020–2027.

Dahmen, T. (2012). Optimization of pacing strategies for cycling time trials using a smooth 6-parameter endurance model. In *Proceedings Pre-Olympic Congress on Sports Science and Computer Science in Sport (IACSS), Liverpool, England, UK, July 24-25, 2012*.

Dahmen, T., Byshko, R., Saupe, D., Röder, M., and Mantler, S. (2011). Validation of a model and a simulator for road cycling on real tracks. *Sports Engineering*, 14(2-4):95–110.

Gaesser, G. A. and Poole, D. C. (1996). The slow component of oxygen uptake kinetics in humans. *Exercise and sport sciences reviews*, 24(1):35–70.

Jones, A. M. and Poole, D. C. (2005). Introduction to oxygen uptake kinetics and historical development of the discipline. In Jones, A. M. and Poole, D. C., editors, *Oxygen Uptake Kinetics in Sport, Exercise and Medicine*, pages 3–35. London: Routledge.

Ma, S., Rossiter, H. B., Barstow, T. J., Casaburi, R., and Porszasz, J. (2010). Clarifying the equation for modeling of $\dot{V}O_2$ kinetics above the lactate threshold. *Journal of Applied Physiology*, 109(4):1283–1284.

Martin, J. C., Milliken, D. L., Cobb, J. E., McFadden, K. L., and Coggan, A. R. (1998). Validation of a mathematical model for road cycling power. *Journal of Applied Biomechanics*, 14:276–291.

Poole, D. C. and Jones, A. M. (2012). Oxygen uptake kinetics. *Comprehensive Physiology*, 2:933–996.

Pringle, J. S. and Jones, A. M. (2002). Maximal lactate steady state, critical power and emg during cycling. *European journal of applied physiology*, 88(3):214–226.

Stirling, J., Zakynthinaki, M., and Billat, V. (2008). Modeling and analysis of the effect of training on $\dot{V}O_2$ kinetics and anaerobic capacity. *Bulletin of Mathematical Biology*, 70(5):1348–1370.

Svedahl, K. and MacIntosh, B. R. (2003). Anaerobic threshold: the concept and methods of measurement. *Canadian Journal of Applied Physiology*, 28(2):299–323.

Vautier, J., Vandewalle, H., Arabi, H., and Monod, H. (1995). Critical power as an endurance index. *Applied ergonomics*, 26(2):117–121.

Whipp, B. J., Ward, S. A., Lamarra, N., Davis, J. A., and Wasserman, K. (1982). Parameters of ventilatory and gas exchange dynamics during exercise. *Journal of Applied Physiology*, 52(6):1506–1513.